



0956-716X(95)00485-8

GRAIN BOUNDARY PRECIPITATION BEHAVIORS IN AN Fe-9.8Al-28.6Mn-0.8Si-1.0C ALLOY

C.Y. Chao, C.N. Hwang and T.F. Liu

Institute of Materials Science and Engineering

National Chiao Tung University

Hsinchu, Taiwan, R.O.C.

(Received February 1, 1995)

Introduction

The phase transformations in Fe-Al-Mn-C alloys have been extensively studied by many workers(1-15). Based on their studies, it is seen that when an alloy with a chemical composition in the range of Fe-(8-11) wt pct Al-(28-35) wt pct Mn-(0.8-1.3) wt pct C was solution heat-treated and then quenched, the microstructure was single austenite (γ) phase. When the as-quenched alloy was aged at temperatures ranging from 550°C to 750°C for short times, fine (Fe,Mn)₃AlC carbides (κ' -phase) having an $L'1_2$ -type structure were observed to appear within the austenite matrix, but not on the austenite grain boundaries. However, when the aging time was increased within this temperature range, a $\gamma \rightarrow \alpha$ (ferrite) + κ transition (12), or a $\gamma \rightarrow \alpha + \beta$ -Mn transition (11-13), or a $\gamma \rightarrow \alpha + \kappa + \beta$ -Mn transition (14) occurred on the austenite grain boundaries. The κ phase is also an (Fe,Mn)₃AlC carbide, which was formed on the grain boundary as a coarse particle(12-14).

Recently, the present workers performed transmission electron microscopy observations on the microstructures of the Fe-9.8Al-28.6Mn-0.8Si-1.0C alloy after being solution heat-treated, quenched and then aged at 600°C(16). In the as-quenched condition, the microstructure of the alloy was single austenite phase. After being aged at 600°C for short times, fine (Fe,Mn)₃AlC carbides were observed within the austenite matrix and no grain boundary precipitates could be detected. This is similar to that found by other workers in the Fe-Al-Mn-C alloys(6-12). However, after prolonged aging at 600°C, a $\gamma \rightarrow D0_3 + \kappa$ transition occurred on the grain boundaries. This transition has never before been observed by other workers in the Fe-Al-Mn-C and Fe-Al-Mn-Si-C alloys(1-15,17-22). Extending the previous study, it is interesting to study successively the microstructures of this alloy after being aged at above 600°C.

Experimental Procedure

The alloy, Fe-9.8wt.% Al-28.6 wt.% Mn-0.8 wt.% Si-1.0 wt.% C, was prepared in an air induction furnace by using iron (99.5%), electrolytic aluminum (99.7%), electrolytic manganese (99.9%), electrolytic silicon (99.9%), and pure carbon powder. After being homogenized at 1250°C for 12 hours under a protective argon atmosphere, the ingot was hot forged and then cold rolled to a final thickness of 1.0 mm. The sheet was subsequently solution heat-treated at 1050°C for 2 hours and rapidly quenched into room-temperature water. The aging processes were performed at temperatures ranging from 620°C to 900°C for various times in a salt bath and then quenched into water.

Specimens for electron microscopy were prepared by means of a double jet electropolisher with an electrolyte of 60 percent ethanol, 30 percent acetic acid, and 10 percent perchloric acid. The polishing temperature was kept in the range from -10 to 10°C , and the current density was kept in the range from 1.5×10^4 to 2.0×10^4 A/m^2 . Electron microscopy was performed on a JEOL 2000FX scanning transmission electron microscope (STEM) operating at 200kV. This microscope was equipped with an energy-dispersive X-ray spectrometer (EDS) for chemical microanalysis.

Results and Discussion

In the as-quenched condition, the microstructure of the alloy was single austenite phase (16). Transmission electron microscopy examinations indicated that when the alloy was aged at 725°C or below, fine $(\text{Fe},\text{Mn})_3\text{AlC}$ carbides were formed within the austenite matrix and the $\gamma \rightarrow \text{D}_0_3 + \kappa$ transition occurred on the austenite grain boundaries. This feature is similar to that found in the alloy aged at 600°C (16). However, when the aging temperature was increased to 750°C , only grain boundary precipitates could be observed and no evidence of precipitates could be detected within the austenite matrix. An example is shown in Figure 1. Figure 1(a) is a bright-field (BF) electron micrograph of the alloy aged at 750°C for 2 hours and then quenched. Electron diffraction showed that the grain boundary precipitates were also a mixture of $(\text{D}_0_3 + \kappa)$ phases. Figure 1(b), a 111 D_0_3 dark-field (DF) electron micrograph of the same area as Figure 1(a), clearly exhibits the presence of the D_0_3 particles. It is noted here that in the present alloy the grain boundary κ carbide was preserved to higher temperature than κ' carbide inside the grain. This result is consistent with that observed by other workers in the Fe-Al-Mn-C alloys(12-14).

Figure 2(a) shows a BF electron micrograph of the alloy aged at 800°C for 1 hour and then quenched, revealing the presence of the grain boundary precipitates. Figure 2(b) is a selected-area diffraction pattern (SADP) taken from an area covering two precipitates marked as K_1 and D_1 in Figure 2(a). Analyses by the SADP indicated that these two precipitates were of the κ carbide and D_0_3 phase, respectively, and the orientation relationship between the κ carbide and D_0_3 phase was $[001]_{\kappa} // [011]_{\text{D}_0_3}$ and $(210)_{\kappa} // (1\bar{1}1)_{\text{D}_0_3}$. This is similar to that found in the alloy aged at 750°C or below(16). Therefore, it is likely to conclude that the $\gamma \rightarrow \kappa + \text{D}_0_3$ transition had also occurred on the austenite grain boundary when the alloy was aged 800°C . However, the 200 D_0_3 (or, equivalently 100 $\text{B}_2(23-24)$) DF electron micrograph of the D_1 precipitate revealed that the whole particle was bright in contrast, as shown in Figure 2(c); whereas the 111 D_0_3 DF electron micrograph of the same particle showed that only small D_0_3 domains were present within this particle (see Figure

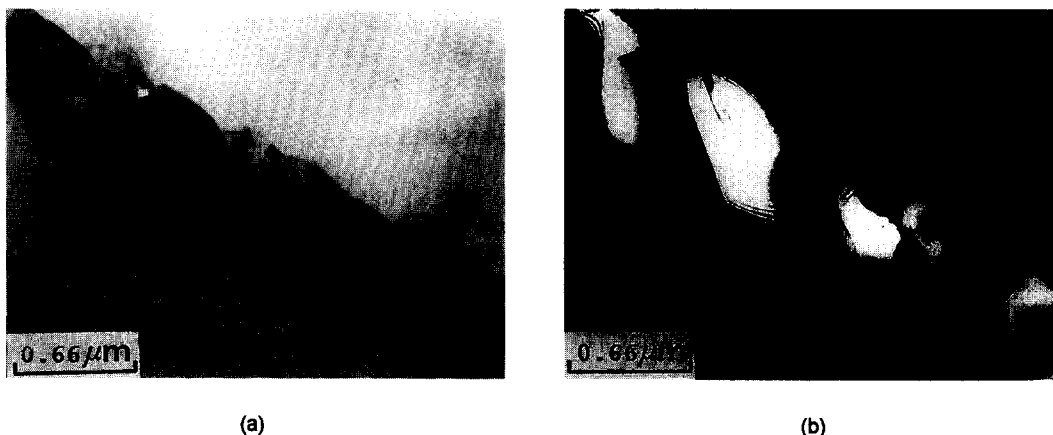
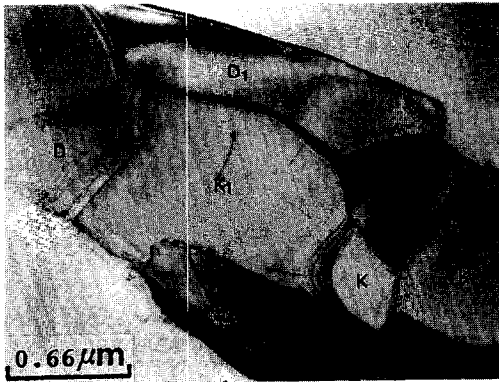


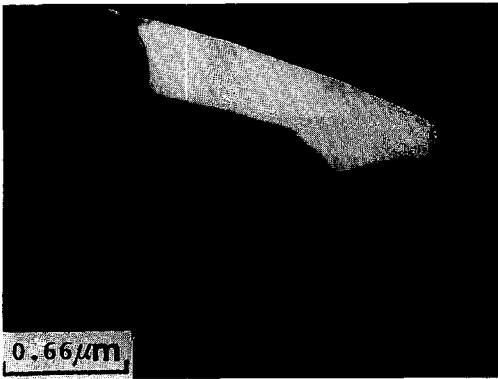
Figure 1. Electron micrographs of the alloy aged 750°C for 2 hours. (a) BF and (b) 111 D_0_3 DF.



(a)



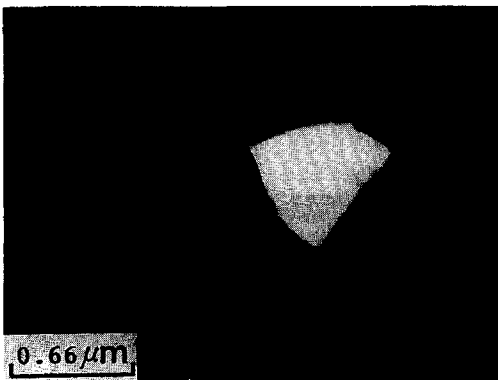
(b)



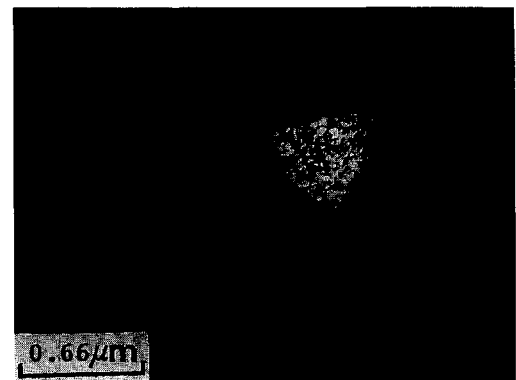
(c)



(d)



(e)



(f)

Figure 2. Electron micrographs of the alloy aged 800°C for 1 hour. (a) BF, (b) a SADP taken from an area covering a coarse κ carbide and a D0, phase. The zone axes of κ carbide and D0, are [001] and [011], respectively ($hkl=\kappa$ carbide; $hkl=D0$, phase). (c) and (d) DF electron micrographs obtained by use of the 200 and 111 D0, reflection, respectively, (e) 200 and (f) 111 D0, DF.

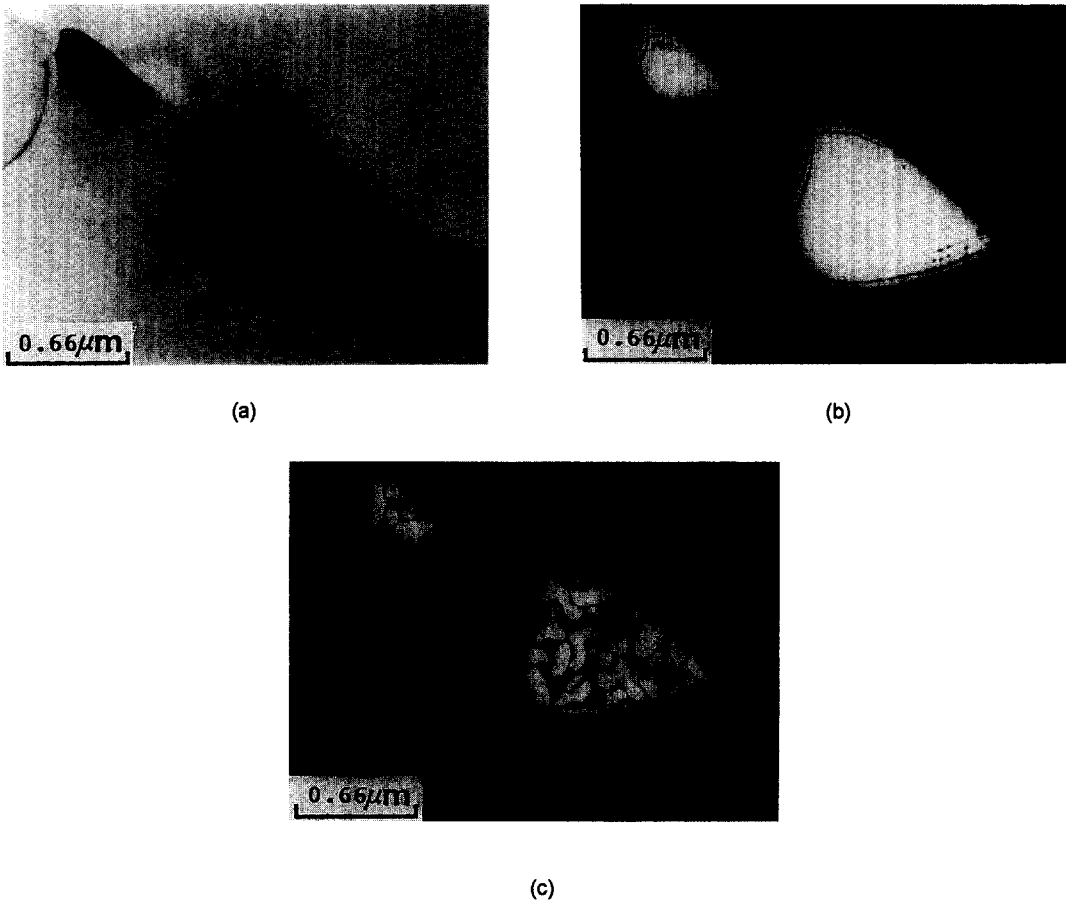


Figure 3. Electron micrographs of the alloy aged at 825°C for 1 hour. (a) BF, (b) 200 and (c) 111 D₀, DF.

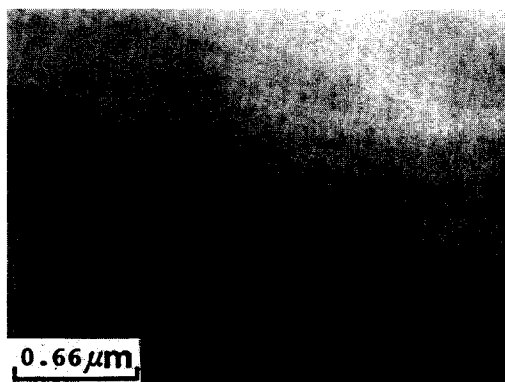


Figure 4. A BF electron micrograph of the alloy aged at 850°C for 2 hours.

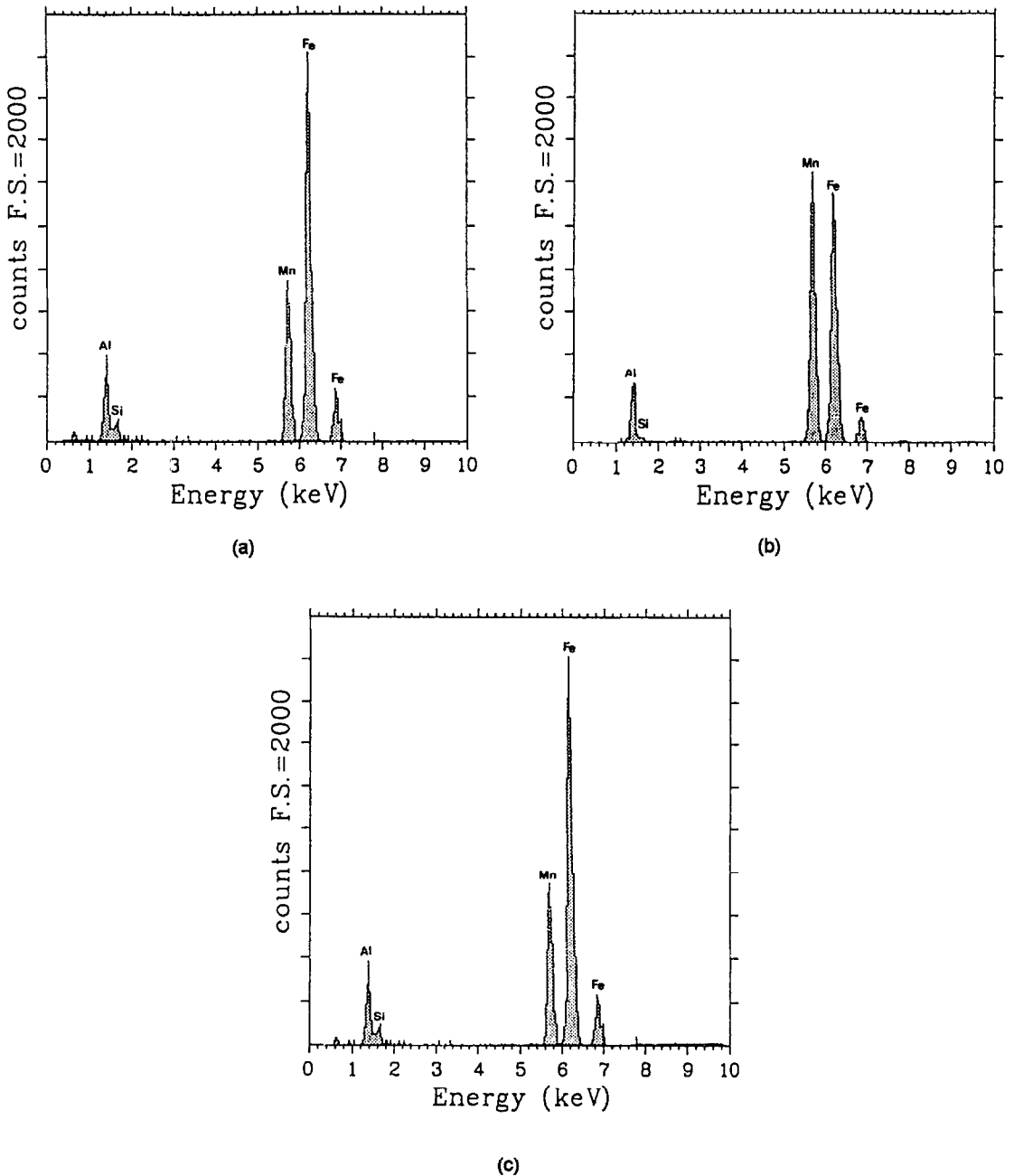


Figure 5. Three typical chemical composition profiles taken from (a) an as-quenched alloy, (b) a coarse κ carbide and (c) a $D0_3$ particle, respectively.

2(d)). This indicates that the microstructure of the particle present at 800°C is B2 phase and the small $D0_3$ domains were formed by a B2 \rightarrow $D0_3$ continuous ordering transition during quenching from the quenching temperature (23-24). Figures 2(e) and (f), the 200 and 111 $D0_3$ DF electron micrographs of the precipitate marked

TABLE 1
Chemical Compositions of the Phases Revealed by
Energy-Dispersive X-ray Spectrometer (EDS)

Heat Treatment	Phase	Chemical Composition (Wt pct)			
		Fe	Al	Mn	Si
1. As-quenched	γ	bal.	9.81	28.60	0.80
2. 800°C aging	κ	bal.	9.46	44.52	0.19
	B2	bal.	10.52	20.03	1.37

as D_2 in Figure 2(a), represent another example of the $B2 \rightarrow D_0_3$ ordering transition. Obviously, a $\gamma \rightarrow B2 + \kappa$ transition had occurred on the austenite grain boundaries in the alloy aged at 800°C.

Shown in Figures 3(a) through (c) are the BF, 200 and 111 D_0_3 DF electron micrographs of the alloy aged at 825°C for 1 hour. In these figures, it is clear that only the B2 precipitates were formed on the austenite grain boundaries. Progressively higher temperature aging and quenching experiments indicated that the grain boundary precipitation of B2 phase was preserved up to 840°C. However, in the alloy aged at 850°C for 2 hours and then quenched, no evidence of precipitates could be detected, as shown in Figure 4. This indicates that the microstructure of the present alloy at 850° or above is single austenite phase.

Based on the above observations, an important experimental result is worthy to discuss. The D_0_3 phase had also been observed in the Fe-Al, Fe-Al-Ti, Fe-Al-Mn and Fe-Al-Mn-C alloys(23-27). In these alloys, it is seen that if the D_0_3 phase was formed by continuous ordering transition during quenching, it was always occurred through a $\alpha \rightarrow B2 \rightarrow D_0_3$ transition. The $\alpha \rightarrow B2$ transition produced $a/4\langle 111 \rangle$ APBs and the $B2 \rightarrow D_0_3$ transition produced $a/2\langle 100 \rangle$ APBs(23-24). However, in the present study, although the D_0_3 phase was also formed during quenching from the aging temperature ranging from 800 to 840°C, no evidence of the ferrite phase could be detected. The reasons may be due to (i) the ferrite phase does not actually exist in the present alloy. (ii) owing to rapid growth of the B2 domains. Figures 5(a) through (c) show three typical chemical composition profiles taken from the as-quenched alloy and a κ carbide as well as a B2 phase in the alloy aged at 800°C for 1 hour, respectively, where only iron, aluminum, manganese and silicon peaks were examined (carbon cannot be examined by the conventional EDS analysis). The quantitative chemical compositions obtained by analyzing ten different EDS profiles of each phase are listed in Table 1. It is clearly seen in Table 1 and Figure 5 that the concentration of silicon in the B2 phase is much greater than that in the κ carbide and austenite matrix. It is well-known that a small amount of silicon addition in binary Fe-Al alloys pronouncedly increased the energy of the $a/4\langle 111 \rangle$ APB(28-29). This may cause the B2 domains to grow up to the whole particle during quenching; therefore, no $a/4\langle 111 \rangle$ APBs could be detected. It means that based on the observations of the quenched-specimens, it is difficult to determine the phase present at temperatures ranging from 800 to 840°C to be B2 or α phase.

In summary, a $\gamma \rightarrow D_0_3 + \kappa$ transition occurred on the austenite grain boundary in the Fe-9.8Al-28.6Mn-0.8Si-1.0C alloy aged at 750°C. When the aging temperature was increased to 800°C, the grain boundary precipitates were a mixture of (B2 + κ) or (α + κ) phases. With increasing the aging temperature to 825°C, only B2 (or α) precipitates could be observed on the austenite grain boundary.

Acknowledgment

The authors are pleased to acknowledge the financial support of this research by the National Science Council, Republic of China, under Grant No. NSC83-0405-E009-003. They are also grateful to Miss M.H. Lin for typing.

References

1. G.L. Kayak: Met. Sci. Heat Treat., **11(2)**, 95. (1969)
2. D.J. Schmatz: Trans. ASM, **52**, 898. (1960)
3. J.C. Benz and H.W. Leavenworth: J. Met., Mar., 36. (1985)
4. S.C. Chang and Y.H. Hsiau: J. Mater. Sci., **24**, 1117. (1989)
5. T.F. Liu and C.M. Wan: Strength Met. Alloys, **1**, 423. (1986)
6. J.E. Krzanowski: Metall. Trans. A, **19A**, 1873. (1988)
7. K.H. Han, J.C. Yoon and W.K. Choo: Scripta Metall., **20**, 33. (1986)
8. K. Sato, K. Tagawa and Y. Inoue: Scripta Metall., **22(6)**, 899. (1988)
9. K. Sato, K. Tagawa and Y. Inoue: Mat. Sci. & Eng., **A111**, 45. (1989)
10. K.H. Han, W.K. Choo and D.E. Laughlin: Scripta Metall., **22(12)**, 1875. (1988)
11. K. Sato, K. Tagawa and Y. Inoue: Metall. Trans. A, **21A**, 5. (1990)
12. W.K. Choo and K.H. Han: Metall. Trans. A, **16A**, 5. (1985)
13. K.H. Han and W.K. Choo: Metall. Trans. A, **20A**, 205. (1989)
14. G.S. Krivonogov, M.F. Alekseyenko and G.G. Solovyeva: Phys. Met. Metall., **34(4)**, 86. (1975)
15. N.A. Storchak and A.G. Drachinskaya: Phys. Met. Metall., **44(2)**, 123. (1977)
16. C.Y. Chao and T.F. Liu: Scripta Metall., **25**, 1623. (1991)
17. S.K. Banerji: Met. Prog., Apr. 59. (1978)
18. R. Wang and F.H. Beck: Met. Prog., Mar. 72. (1983)
19. U. Bernabai, G.A. Capuano, A. Dang and F. Felli: Oxid. Met., **33**, 309. (1990)
20. J.P. Sauer, R.A. Rapp and J.P. Hirth: Oxid. Met., **18**, 285. (1982)
21. J.C. Garcia, N. Rosas and R.J. Rioja: Met. Prog., Aug. 47. (1982)
22. J.S. Dunning, M.L. Glenn and H.W. Leavenworth, Jr.: Met. Prog., Oct., 19. (1984)
23. S.M. Allen and J.W. Cahn: Acta Metall., **24**, 425. (1976)
24. P.R. Swann, W.R. Duff and R.M. Fisher: Metall. Trans. A, **3**, 409. (1972)
25. M.G. Mendiratta, S.K. Ehlers and H.A. Lipsitt: Metall. Trans. A, **18A**, 509. (1987)
26. V.P. Zalutskiy, Y.G. Nesterenko and I.A. Osipenko: Fiz. Met. Metalloved., **39(5)**, 1026 (1975)
27. C.C. Wu, J.S. Chou and T.F. Liu: Metall. Trans. A, **22A**, 2265. (1991)
28. M.G. Mendiratta and S.K. Ehlers: Metall. Trans. A, **14A**, 2435. (1983)
29. Y.J. Chang: Acta Metall., **30**, 1185. (1982)